
MiniBooNE first results on a search for ν_e appearance at the $\Delta m^2 \sim 1 \text{ eV}^2$ scale

M. Sorel¹, on behalf of the MiniBooNE Collaboration

Columbia University, New York, NY 10027, USA sorel@ific.uv.es [†]

1 Introduction

Solar and atmospheric neutrino oscillations, recently confirmed by reactor and accelerator-based experiments, are now well established. On the other hand, the interpretation of the LSND $\bar{\nu}_e$ excess [1] as $\bar{\nu}_\mu \rightarrow \bar{\nu}_e$ oscillations at the $\Delta m^2 \sim 1 \text{ eV}^2$ scale lacked for many years experimental confirmation or refutation. The primary goal of the MiniBooNE experiment [2] is to address this anomaly in an unambiguous and independent way.

The MiniBooNE flux is obtained via a high-intensity, conventional neutrino beam. Secondary hadrons, mostly pions and kaons, are produced via the interactions of 8 GeV protons from the Fermilab Booster accelerator with a thick beryllium target, and are focused by a horn. The switchable horn polarity allows for both neutrino and antineutrino running modes. The neutrino beam is produced via the decay of secondary mesons and muons in a 50 m long decay region. Overall, about $9.5 \cdot 10^{20}$ protons on target have been accumulated over the five years of beamline operation, $5.6 \cdot 10^{20}$ of which are used in this oscillation analysis, based on the neutrino running mode sample only.

The MiniBooNE detector is located 540 m away from the beryllium target. The detector is a 12 m in diameter sphere filled with 800 t of undoped mineral oil, whose inner region is instrumented with 1280 photomultiplier tubes (PMTs). Neutrino interactions produce prompt, ring-distributed Cherenkov light, and delayed, isotropic scintillation light. Light transmission is affected by fluorescence, scattering, absorption and reflections. The outer detector region is used to reject cosmic ray activity or uncontained neutrino interactions. About $7.7 \cdot 10^5$ neutrino interactions have been collected at MiniBooNE.

The goal of the first MiniBooNE electron appearance analysis is two-fold: perform a model-independent search for a ν_e excess (or deficit), and interpret the data within a two neutrino, appearance-only $\nu_\mu \rightarrow \nu_e$ oscillation context, to test this interpretation of the LSND anomaly [2]. This was a blind analysis.

[†] Present address: IFIC, CSIC and Universidad de Valencia, Spain

2 The closed electron neutrino box era

Expectations for ν_e candidate events are formed by simulating neutrino fluxes, neutrino interactions, and detector response. Parametrizations of pion [3] and kaon [4] production data on beryllium are the most important external physics input to the GEANT4 [5] beamline description. The ν_μ flux is dominated by $\pi^+ \rightarrow \mu^+ \nu_\mu$ decays, with a high-energy tail due to $K^+ \rightarrow \mu^+ \nu_\mu$. The ν_e flux is mostly due to $\mu^+ \rightarrow \bar{\nu}_e e^+ \nu_e$ and $K^+ \rightarrow \pi^0 e^+ \nu_e$. The flux-averaged neutrino energy and the ν_e/ν_μ flux ratio are about 0.8 GeV and 0.5%, respectively. Neutrino interactions are simulated with the NUANCEv3 [6] code, describing all relevant neutrino interaction processes and carbon target nuclear effects, with modifications partly based on MiniBooNE neutrino data [2, 7, 8]. At MiniBooNE, 39%, 25% and 8% of all neutrino interactions are expected to proceed via charged current quasi-elastic (CCQE) scattering, charged current π^\pm production and neutral current (NC) π^0 production, respectively. The GEANT3 [9] detector response simulation includes a detailed modeling of light production and transmission mechanisms [10], and of the PMT charge/time response. The detector calibration makes use of tabletop measurements of mineral oil optical properties, MiniBooNE laser calibration data, Michel electron tracks from muon decays at rest, and NC neutrino interactions. The calibration is validated using cosmic muons, ν_μ interactions, and ν_e interactions from the NuMI beamline.

A detailed model of extended-track light production and propagation is used to reconstruct neutrino interactions [2]. A first event selection for the appearance analysis is performed via hit multiplicity, fiducial volume, and energy threshold requirements. A higher-level selection based on particle identification is applied next, to reject final state muons and π^0 's, and enhance the CCQE fraction in the ν_e sample. For this purpose, each event is reconstructed under four hypotheses: single muon track, single electron track, two track with invariant mass fixed to the π^0 mass, and unconstrained two track hypothesis, returning L_μ , L_e , L_π likelihood fit values and a $m_{\gamma\gamma}$ invariant mass value, respectively. The cut values in L_e/L_μ , L_e/L_π and $m_{\gamma\gamma}$ are energy-dependent, and chosen to optimize the $\nu_\mu \rightarrow \nu_e$ sensitivity.

About half of the backgrounds to the oscillation signal in the final sample are expected to be due to the ν_e contamination in the ν_μ beam, with roughly the other half due to mis-identified ν_μ interactions. One of the strengths of the MiniBooNE appearance analysis is that all relevant backgrounds can be directly constrained or cross-checked via MiniBooNE data samples other than the ν_e candidate sample. The main mis-identification background, due to $\nu_\mu N \rightarrow \nu_\mu N \pi^0$ interactions where one of the two photons from the π^0 decay is not seen, is constrained using a high-purity sample of NC π^0 interactions. Neutrino beam interactions with material surrounding the detector, creating 100-300 MeV photons that penetrate the detector unvetoes, can also be mis-identified as ν_e events. Using a sample of high detector radius, inward-pointing events, this background expectation is confirmed with data with an

accuracy of about 15%. The most important intrinsic ν_e background is due to $\mu^+ \rightarrow \bar{\nu}_\mu \nu_e e^+$ decays, and can be accurately constrained via ν_μ CCQE events. Finally, for what concerns the intrinsic ν_e background due to kaon decay, the kaon-induced flux is directly measured at high energies, where no significant oscillation events are expected, and then extrapolated to lower energies [2].

Systematic errors in predicting ν_e candidate events, due to uncertainties in the modeling of the beam, neutrino interactions, and detector response, have been thoroughly evaluated. A first estimate is obtained from “first principles” uncertainties from simulation models and external measurements. Better estimates are obtained via MiniBooNE calibration and neutrino data fits. Extensive cross-checks on a variety of distributions and open data samples insensitive to oscillations have been performed prior to box opening, to quantitatively verify the good level of agreement between data and predictions.

3 The open electron neutrino box era

Box opening proceeded as follows. First, a neutrino oscillation fit of the neutrino energy distribution for ν_e -like events in the $300 < E_\nu < 3000$ MeV energy range is performed, retaining blindness to the best-fit oscillation signal component added to background predictions. Goodness-of-fit information from the comparison of data with Monte Carlo (MC) predictions in several diagnostic variables is disclosed. Second, data and MC histogram contents for the same diagnostic variables is disclosed. Third, goodness-of-fit information from the neutrino energy distribution data/MC comparison is disclosed. Fourth, full information on ν_e candidate events and oscillation fit results is disclosed. This scheme allowed to progress in a step-wise fashion, with ability to iterate if necessary. All event selection and oscillation fit procedures were determined before full box opening.

In a first iteration, comparisons between data and predictions were satisfactory in all diagnostic variables except for the visible energy, which returned a χ^2 probability of 1%, indicating a poor data/MC agreement beyond the ability of a two neutrino, appearance-only oscillation model to handle. This triggered further investigations of background estimates and associated uncertainties, but no evidence of a problem was found. However, given that backgrounds rise at low energies, that studies focused suspicions in the low-energy region, and that this choice has negligible impact on the oscillation sensitivity, the MiniBooNE Collaboration decided to look for an oscillation signal in the reduced $475 < E_\nu < 3000$ MeV range, while reporting electron candidate events over the full $300 < E_\nu < 3000$ MeV range. With the oscillation analysis energy threshold increased, a second box opening iteration indicated good data/MC agreement in all diagnostic variables. No oddities in any of the subsequent box opening steps were found, and electron candidate events became fully unblinded.

MiniBooNE observes 380 electron candidate events in the $475 < E_\nu < 1250$ MeV energy range, to be compared with a no-oscillation background prediction of $358 \pm 19 \pm 35$. No evidence for neutrino oscillations is found. The same conclusion is reached by performing a fit to the neutrino energy distribution (see Fig.1) over the $475 < E_\nu < 3000$ MeV range: the no-oscillation hypothesis describes the data well, with a goodness-of-fit $\chi^2/\text{dof} \simeq 1.8/8$, and no statistically significant differences in the description of the data are found assuming oscillations. Given the null result, an upper limit on neutrino oscillations is obtained. As shown in Fig. 1, no overlap in the 90% confidence level regions in oscillation parameter space allowed by MiniBooNE and LSND exists. MiniBooNE excludes two neutrino appearance-only oscillations as the explanation of the LSND anomaly at 98% confidence level. Very similar results are obtained with a second, largely independent, analysis [2].

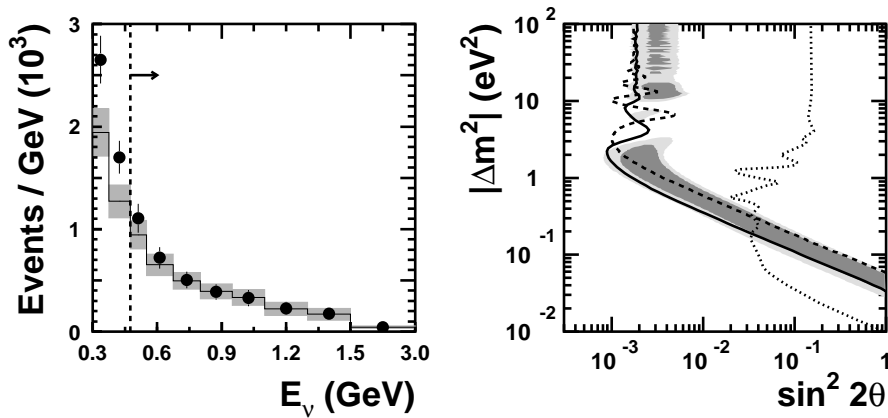


Fig. 1. Left: ν_e candidate events versus reconstructed neutrino energy E_ν [2]. Points indicate data with statistical-only error bars. The histogram shows the total background expectation, with systematic-only error rectangles. Right: allowed regions in oscillation parameter space ($|\Delta m^2|$, $\sin^2 2\theta$). The filled regions indicate the region allowed by LSND [1] at 90 and 99% confidence level. The solid, dashed, and dotted curves indicate the 90% confidence level upper limits from the MiniBooNE [2], KARMEN [11], and Bugey [12] experiments, respectively.

Upon investigation of electron candidate events over the full, $300 < E_\nu < 3000$ MeV, energy range (see Fig. 1), it is found that low-energy data do not match expectations. A 3.7σ excess is seen in the data for $300 < E_\nu < 475$ MeV. This discrepancy is currently not understood and under investigation. While this low-energy excess does not seem consistent with two neutrino appearance-only oscillations, more studies are needed to clarify its causes.

4 Conclusions and outlook

In conclusion, MiniBooNE finds excellent agreement between data and no-oscillation predictions in the oscillation analysis energy range. As a consequence, and if neutrino and antineutrino oscillations are the same, MiniBooNE excludes at 98% confidence level the two neutrino, appearance-only $\nu_\mu \rightarrow \nu_e$ oscillations interpretation of the LSND anomaly. For energies below the oscillation analysis range, MiniBooNE finds an excess of electron candidate events above expectations that is currently not understood and under investigation.

Apart from understanding this low-energy discrepancy, MiniBooNE's near-term goals include an improvement in oscillation sensitivity by combining the merits of the two analyses developed for this first result, additional searches addressing different models explaining the LSND anomaly, and neutrino cross section measurements. Results from the MiniBooNE's ongoing antineutrino running are expected after that.

The MiniBooNE Collaboration acknowledges the support of Fermilab, the US Department of Energy, and the US National Science Foundation. The author is supported by a Marie Curie Intra-European Fellowship within the 6th European Community Framework Program.

References

1. A. Aguilar et al [LSND Collaboration]: Phys. Rev. D **64**, 112007 (2001) [arXiv:hep-ex/0104049]
2. A. A. Aguilar-Arevalo et al [MiniBooNE Collaboration]: Phys. Rev. Lett. **98**, 231801 (2007) [arXiv:0704.1500 [hep-ex]]
3. M. G. Catanesi et al [HARP Collaboration]: Eur. Phys. J. C **52**, 29 (2007) [arXiv:hep-ex/0702024]. I. Chemakin et al [E910 Collaboration]: arXiv:0707.2375 [nucl-ex]
4. T. Abbott et al [E-802 Collaboration]: Phys. Rev. D **45**, 3906 (1992); A. Aleshin et al: ITEP-77-80 (1977); J. V. Allaby et al: CERN-70-12 (1970); D. Dekkers et al: Phys. Rev. **137**, B962 (1965); T. Eichten et al: Nucl. Phys. B **44**, 333 (1972); I. A. Vorontsov et al: ITEP-88-11 (1988).
5. S. Agostinelli et al [GEANT4 Collaboration]: Nucl. Instrum. Meth. A **506**, 250 (2003)
6. D. Casper, Nucl. Phys. Proc. Suppl. **112**, 161 (2002) [arXiv:hep-ph/0208030].
7. A. A. Aguilar-Arevalo et al [MiniBooNE Collaboration]: arXiv:0706.0926 [hep-ex].
8. D. Ashery et al: Phys. Rev. C **23**, 2173 (1981); H. Ejiri, Phys. Rev. C **48**, 1442 (1993); D. Rein and L. M. Sehgal, Annals Phys. **133**, 79 (1981)
9. CERN Program Library Long Writeup W5013 (1993)
10. B. C. Brown et al: IEEE Nuclear Science Symposium Conference Record 1, 652 (2004)
11. B. Armbruster et al [KARMEN Collaboration]: Phys. Rev. D **65**, 112001 (2002) [arXiv:hep-ex/0203021]
12. Y. Declais et al: Nucl. Phys. B **434**, 503 (1995)